THE UNIVERSITY OF MICHIGAN

COLLEGE OF ENGINEERING

DEPARTMENT OF ELECTRICAL ENGINEERING & COMPUTER SCIENCE

Radiation Laboratory

Scattering by a Two Dimensional Groove in a Ground Plane

K. Barkeshli and J.L. Volakis

The Radiation Laboratory
Department of Electrical Engineering
and Computer Science
The University of Michigan
Ann Arbor, MI 48109-2122

February 1989

National Aeronautics and
Space Administration
Ames Research Center
Moffett Field, CA 94035
Grant NAG-2-541

Ann Arbor, Michigan

TECHNICAL REPORT

FOR

NASA Grant NAG-2-541

Grant Title: A NEW TECHNIQUE FOR SIMULATING COMPOSITE MATERIAL
Task 4: Numerical Implementation of Generalized Impedance Boundary Conditions

Institution: The Radiation Laboratory
Department of Electrical Engineering
and Computer Science
The University of Michigan
Ann Arbor, MI 48109-2122

Period Covered: September 1988 - February 1989

Report Title: Scattering by a Two Dimensional Groove in a Ground Plane

Report Authors: K. Barkeshli and J. L. Volakis

Principle Investigator: John L. Volakis
Telephone: (313) 764-0500

Table of Contents

Scattering by a Two Dimensional Groove in a Ground Plane

Kasra Barkeshli and John L. Volakis

Abstract

Higher order boundary conditions involve derivatives of the fields beyond the first and were recently shown to be more effective than traditional first order conditions in modeling dielectric coatings and layers. In this report an application of a third order generalized boundary condition to scattering by a filled rectangular groove is presented. Deficiencies of such higher order boundary conditions are addressed and a correction is proposed for the present case. As part of the process of examining and improving the accuracy of the proposed generalized boundary conditions, an exact solution is developed and a comparison is provided with a solution based on the standard impedance boundary condition.

I. INTRODUCTION

Traditionally, the standard impedance boundary condition (SIBC) [1] has been employed to simulate thin material layers on perfectly conducting objects. As is well known, however, the SIBC provides limited accuracy and is particularly applicable to lossy and/or high contrast dielectrics. This is primarily because it cannot model the polarization current components that are normal to the dielectric layer. As a result, the SIBC has been found to be best suited for near normal incidence, unless the coating's material properties are such that limit penetration within the material.

The SIBC is a first order condition in that its definition involves a single normal derivative of the component of the field normal to the modeled surface. Recently[2], however, a class of boundary conditions were proposed whose major characteristic is the inclusion of higher order derivatives (along the direction of the surface normal) of the normal field components. These were originally introduced by Karp and Karal [3] and Wienstein [4] to simulate surface wave effects, but have been found to be rather general in nature. In fact, they can be employed to simulate any material profile with a suitable choice of the (constant) derivative coefficients. Appropriately, they are referred to a generalized impedance boundary conditions (GIBC) and can be written either in terms of tangential or normal derivatives provided a duality condition is satisfied [2]. Unlike the SIBC they offer several degrees of freedom and allow an accurate prediction of the surface reflected fields at oblique incidences. This was demonstrated in [2] for the infinite planar surface formed by a uniform dielectric layer on a ground plane. It was found that the maximum coating or layer thickness that can

be simulated accurately with a given GIBC was analogous to the highest order derivative included in the condition.

The GIBCs offer several advantages in both asymptotic and numerical analysis of electromagnetic problems. For example, in the case of asymptotic/high frequency analysis, they allow an accurate replacement of a coating on a layer with a sheet boundary condition amenable to a Wiener-Hopf analysis [5,6] or some other function theoretic approach [7]. In numerical analysis, the profile of a coating can be replaced by a simple boundary condition on the surface of the coating. This eliminates a need for introducing unknown polarization currents within the coating or material layer and thus leading to a more efficient solution.

In this report we examine a numerical application of a third order GIBC for scattering by a material filled groove in a ground plane. Since the GIBCs were derived for a coating without terminations, of particular interest in this study is the examination of their accuracy near those terminations. It is, unfortunately, found that they must be supplemented by more accurate conditions in the vicinity of material discontinuities. A procedure is, therefore, introduced that combines the exact and GIBC formulations. Since the exact solution is required for comparison purposes and in developing the hybrid formulation, it is presented in the first part of the report. This is followed by a discussion on the limitations of a formulation based on the SIBC. The integral equation based on a third order GIBC is presented next. This is solved by the conjugate gradient FFT method having an O(N) memory requirement. In contrast, the exact integral equation is not amenable to such a solution and must be solved by a matrix inversion approach having an $O(N^2)$ memory requirement. The hybrid

formulation is presented last and results are given which show the validity of the procedure as well as its limitations.

II. EXACT SOLUTION

A. Formulation

Consider the H_z polarized wave

$$\overline{H}^{i} = \hat{z}\, e^{jk_0\left[(x-\frac{w}{2})\cos\phi_0 + y\sin\phi_0\right]} \tag{1}$$

incident on the two dimensional cavity as shown in Fig. 1 and we are interested in computing the sattered field. The exact formulation for a slit in a ground plane has been developed in [8] and a similar formulation can be followed in the case of the groove. Below we develop an exact integral equation based on this procedure.

In accordance with the equivalence principle the cavity may be closed by a perfect conductor and the equivalent magnetic current

$$\overline{M} = \overline{E} \times \hat{n} \qquad \text{or} \qquad M_z = E_x$$

may then be introduced on the cavity's top surface, where E_x is the x component of the total electric field at the aperture. Referring to Fig. 2 and applying continuity of the tangential electric field across the aperture, we have

$$\bar{E} \times \hat{n} = \bar{E} \times \hat{n}'$$

$$\hat{z}\, M_z = -\hat{z}\, M'_z \qquad (2)$$

$$M'_z = -M_z$$

In addition, continuity of the total tangential magnetic field across the aperture gives

$$H_t^i + H_t^o (M_z) = H_t^b (M'_z) = H_t^b (-M_z) = -H_t^b (M_z) \quad ; \; y = 0^+ \qquad (3)$$

in which H_t^b denotes the tangential magnetic field at the cavity's surface in region b and likewise H_t^o is the tangential field at $y = 0^+$.

From (3) an integral equation can be obtained after substitution of the appropriate field expressions. On the aperture (y=0), these are

$$H_t^i = 2e^{jk(x-\frac{w}{2})\cos\phi_o} \qquad (4)$$

$$H_t^a (M_z) = -jk_o Y_o \int_0^w 2\, M_z (x')\, G(x, x')\, dx'$$

$$= -\frac{k_o Y_o}{2} \int_0^w M_z (x')\, H_o^{(2)} (k_o |x - x'|)\, dx' \qquad (5)$$

in which $Y_o = 1/Z_o$ is the free space admittance and k_o is the free space wavenumber and a factor of two has been introduced due to image theory.

To find an expression for $H_t^b (M_z)$ we require the cavity Green's function. To find it we proceed as follows: Set

$$\bar{M} = \hat{z}\, M'_z \tag{6}$$

$$\bar{F} = \Psi\, \hat{z} \tag{7}$$

where Ψ is the scalar wave potential satisfying the two dimensional wave equation in the source free region

$$\left(\frac{\partial^2}{\partial x^2} + \frac{\partial^2}{\partial y^2} + k_b^2\right)\Psi = 0 \quad \text{in region b except y = 0.} \tag{8}$$

subject to the appropriate boundary conditions. Also

$$\bar{E} = -\nabla \times \bar{F}\,\hat{x}\frac{\partial}{\partial y}\Psi - \hat{y}\frac{\partial}{\partial x}\Psi \tag{9}$$

$$\bar{H} = -jk_b Y_b \bar{F} \tag{10}$$

in which $Y_b = Y_o\sqrt{\frac{\varepsilon_b}{\mu_b}}$, $k_b = k_o\sqrt{\varepsilon_b \mu_b}$ and (ε_b, μ_b) are the relative constitutive parameters of the material filling the cavity. The scalar wave potential Ψ can be determined by recalling the boundary conditions for the tangential electric field on the walls of the cavity. These are

$$E_x(x, 0) = -M_z \quad \Rightarrow \quad \frac{\partial}{\partial y}\Psi\Big|_{y=0} = -M_z \tag{11}$$

$$E_x(x, -t) = 0 \quad \Rightarrow \quad \frac{\partial}{\partial y}\Psi\Big|_{y=-t} = 0 \tag{12}$$

$$\left.\begin{aligned} E_y(0, y) &= 0 \\ E_y(w, y) &= 0 \end{aligned}\right\} \quad \Rightarrow \quad \frac{\partial}{\partial x}\Psi\Big|_{x=0,\,w} = 0\,. \tag{13}$$

Choosing,

$$\Psi(x, y) = \sum_{p=0}^{\infty} A_p \cos\left[k_p (y + t)\right] \cos \frac{p\pi x}{w} \quad ; \; k_p = \sqrt{k_b^2 - \left(\frac{p\pi}{w}\right)^2}$$

satisfies (12) and (13). The constants A_p are then determined to satisfy (11). That is

$$\frac{\partial \Psi}{\partial y}\Big|_{y=0} = - \sum_{p=0}^{\infty} A_p k_p \sin\left[k_p (y + t)\right] \cos \frac{p\pi x}{w}\Big|_{y=0} = - M_z \tag{14}$$

$$= - \sum_{p=0}^{\infty} A_p k_p \sin (k_p t) \cos \frac{p\pi x}{w} = - M_z .$$

Multiplying both sides by $\cos \frac{q\pi x}{w}$ and integrating, we have

$$- \sum_{p=0}^{\infty} A_p k_p \sin k_p t \int_0^w \cos \frac{p\pi w}{x} \cos \frac{q\pi w}{x} \, dx = - \int_0^w M_z(x) \cos \frac{q\pi}{w} \, dx \tag{15}$$

yielding

$$A_p = \frac{\varepsilon_p}{w k_p \sin k_p t} \int_0^w M_z (x) \cos \frac{p\pi x}{w} \, dx \tag{16}$$

in which

$$\varepsilon_p = \begin{cases} 1 & p = 0 \\ 2 & p > 0 \end{cases}$$

Therefore,

$$H_t^b (M_z) = - j k_b Y_b \sum_{p=0}^{\infty} \frac{\varepsilon_p}{w k_p \sin k_p t} \left[\int_0^w M_z (x') \cos \left(\frac{p\pi x'}{w}\right) dx' \right] \cos\left[k_p (y + t)\right] \cos \left(\frac{p\pi x}{w}\right) \tag{17}$$

B. Moment Method Solution

Substituting (4), (5) and (17) into (3) yields the integral equation

$$\frac{k_o Y_o}{2}\int_0^w M_z(x')\,H_o^{(2)}(k_o|x-x'|)\,dx' - j\frac{k_b Y_b}{w}\sum_{p=0}^{\infty}\frac{\varepsilon_p}{k_p \tan(k_p t)}\cos\frac{p\pi x}{w}\int_0^w M_z(x')\cos\frac{p\pi x'}{w}\,dx'$$

$$= 2\,e^{jk\left(x-\frac{w}{z}\right)\cos\phi_o} \qquad (18)$$

To discretize the above integral equation we expand the magnetuc current in terms of pulses basis function as

$$M_z(x) = \sum_{n=1}^{N} C_n M_n(x) \;;\quad M_n(x) = \begin{cases} 1 & x_n - \frac{\Delta}{2} < x < x_n + \frac{\Delta}{2} \\ 0 & \text{, else} \end{cases} \qquad (19)$$

and by substitution back into (18), we obtain

$$\frac{k_o Y_o}{2}\sum_{n=1}^{N} C_n \int_{x_n-\frac{\Delta}{2}}^{x_n+\frac{\Delta}{2}} H_o^{(2)}(k_o|x-x'|)\,dx' - \frac{jk_b Y_b}{w}\sum_{p=0}^{\infty}\frac{\varepsilon_p}{k_p \tan k_p t}\cos\frac{p\pi x}{w}\sum_{n=1}^{N} C_n \int_{x_n-\frac{\Delta}{2}}^{x_n+\frac{\Delta}{2}}\cos\frac{p\pi x'}{w}\,dx'$$

$$= 2e^{jk\left(x-\frac{w}{2}\right)\cos\phi_o} \qquad (20)$$

Employing point matching, this can now be written as

$$[Y_{mn}]\,[C_n] = [V_m] \tag{21}$$

where

$$Y_{mn} = \frac{k_o Y_o}{4} \int_{x_n - \frac{\Delta}{2}}^{x_n + \frac{\Delta}{2}} H_o^{(2)} (k_o |x_m - x'|)\, dx' - \frac{jk_b Y_b}{2w} \sum_{p=0}^{\infty} \frac{\varepsilon_p \cos\left(\frac{p\pi x_m}{w}\right)}{k_p \tan (k_p t)} \int_{x_n - \frac{\Delta}{2}}^{x_n + \frac{\Delta}{2}} \cos\left(\frac{p\pi x'}{w}\right) dx' \tag{22}$$

and

$$V_m = e^{jk\left(x_m - \frac{w}{2}\right)\cos\phi_o} \tag{23}$$

with $x_m = \frac{m\Delta}{2}$, $m = 1, 2, 3, \ldots$ The elements of the square admittance matrix can be further simplified to

$$Y_{mn} = Y_{mn}^{1} + Y_{mn}^{2} \tag{24}$$

with

$$Y_{mn}^{1} \simeq \begin{cases} \frac{k_o Y_o}{4} \Delta \left[1 - \frac{j2}{\pi} \left(\ln \frac{k_o \Delta}{4} + \gamma - 1\right)\right] & \text{for } n = m \\ \frac{k_o Y_o}{4} \Delta\, H_o^{(2)} (k_o |x_m - x_n|) & \text{for } n \neq m \end{cases} \tag{25a}$$

and

$$Y_{mn}^{2} = -\frac{jk_b y_b}{2w}\,\Delta \sum_{p=0}^{\infty} \frac{\varepsilon_p \cos\left(\frac{p\pi x_m}{w}\right)}{k_p \tan(k_p t)} \cos\frac{p\pi x_n}{w}\ \mathrm{sinc}\frac{p\pi\Delta}{2w}. \qquad (25b)$$

in which γ=0.5772 is the Euler constant.

C. TE Scattering from a Narrow Groove

In this section we examine the exact formulation and compare it to that obtained via application of the standard impedance boundary condition for a narrow groove. By rewriting the integral equation (18) as

$$\frac{k_o y_o}{2} \int_0^w M_z(x')\, H_o^{(2)}(k_o\,|x-x'|)\,dx' + \frac{1}{jwZ_b \tan k_b t} \int_0^w M_z(x')\,dx'$$

$$-j\frac{k_b Y_b}{w} \sum_{p=1}^{\infty} \frac{2}{k_p \tan k_p t} \cos\frac{p\pi x}{w} \int_0^w M_z(x') \cos\frac{p\pi x'}{w}\,dx' = 2e^{jk\left(x-\frac{w}{2}\right)\cos\phi_o} \qquad (26)$$

and setting $\eta_b = jZ_b \tan(k_b t)$ we obtain

$$\frac{k_o Y_o}{2} \int_0^w M_z(x')\, H_o^{(2)}(k_o\,|x-x'|)\,dx' + \frac{1}{w\eta_b} \int_0^w M_z(x')\,dx' = 2e^{jk\left(x-\frac{w}{2}\right)\cos\phi_o} \qquad (27)$$

where we have included only the dominant mode (p=0) in the representation of the cavitiy's Green's function. If we further assume a constant tangential electric field variation ($M_z(x)$ ~ constant) over the aperture, (27) reduces to

$$\frac{k_o y_o}{2} \int_0^w M_z(x')\, H_o^{(2)}(k_o\,|x-x'|)\,dx' + \frac{1}{\eta_b} M_z(x) = 2e^{jk\left(x-\frac{w}{2}\right)\cos\phi_o} \qquad (28)$$

which is the integral equation resulting from an application of the standard impedance boundary condition (SIBC).

The approximations required to go from (26) to (28) are not obviously expected to hold unless the groove is small in depth and width, say $k_o w \leq 0.6$ and $k_o t \leq 0.6$. Consequently one does not expect the SIBC to provide a good simulation of the cavity scattering, particularly near grazing incidences where $M_z(x)$ in not symmetric and may have rapid spatial variation. In fact, it may also be observed that the SIBC integral equation , at best, yields the average of the actual equivalent current distribution on the surface of the crack. This is clearly illustrated in Fig. 3 where the currents and echowidth predicted via (28) and the exact integral equation (20) are compared. The result shown in Fig. 3 is a typical situation and it is not surprising that the backscatter echowidth predicted by the SIBC formulation is in substantial error at oblique incidences.

III. FORMULATION WITH GENERALIZED IMPEDANCE BOUNDARY CONDITIONS

It is desirable to work with a formulation (or an integral equation) that is amenable to a conjugate gradient FFT (CGFFT) implementation. The CGFFT has an $O(N)$ memory requirement and can thus be suitable for treating large size grooves or cavities, particularly when applied to three dimensional geometries. Unfortunately, the exact formulation, in addition to being restricted to rectangular grooves and cracks, is

not suitable for a CGFFT implementation. On the other hand the integral equation (20) resulting from an application of the SIBC, a first order condition, although amenable to a CGFFT is not of acceptable accuracy. Recently, however, higher order impedance boundary conditions involving field derivatives beyond the first have been found to provide a substantially better simulation for fairly thick dielectric coatings. These are referred to as generalized impedance boundary conditions (GIBCs) and take the form

$$\sum_{m=0}^{M} \frac{a_m}{(-jk_o)^m} \frac{\partial^m E_y}{\partial y^m} = 0 \tag{30a}$$

$$\sum_{m=0}^{M} \frac{a'_m}{(-jk_o)^m} \frac{\partial^m H_y}{\partial y^m} = 0 \tag{30b}$$

where a_m and a'_m are constants specific to the surface, layer or coating being modeled. For M=1, they reduce to the SIBC provided we set

$$Z_b = \eta_b Z_o = j \frac{Z_o N}{\varepsilon_b} \tan(k_b t) = \frac{a_0}{a_1} = \frac{a'_1}{a'_0} \tag{31}$$

where $N = \sqrt{\mu_b \varepsilon_b}$. A third order GIBC corresponds to M=3. In that case, an accurate simulation of the reflection coefficient for a metal-backed uniform dielectric layer can be obtained by choosing

$$a_0 = (N - \frac{1}{2N})\left[\tan(ktN) - \tan(\frac{kt}{2N})\right]$$

$$a_1 = i\varepsilon_b\left[1 + \tan(ktN)\tan(\frac{kt}{2N})\right]$$

$$a_2 = \frac{1}{2N}\left\{\tan(ktN) - \tan(\frac{kt}{2N}) + kt(N - \frac{1}{2N})\left[1 + \tan(ktN)\tan(\frac{kt}{2N})\right]\right\} \quad (32)$$

$$a_3 = -\frac{ikt\varepsilon_b}{2N}\left[\tan(ktN) - \tan(\frac{kt}{2N})\right]$$

and

$$a'_0 = (2N^2 - 1)\left[1 + \cos(ktN)\cot(\frac{kt}{2N})\right]$$

$$a'_1 = 1\ 2N\mu_b\left[\cot(ktN) - \cot(\frac{kt}{2N})\right]$$

$$a'_2 = 1 + \cot(ktN)\cot(\frac{kt}{2N}) + kt(N - \frac{1}{2N})\left[\cot(ktN) - \cot(\frac{kt}{2N})\right] \quad (33)$$

$$a'_3 = -i\ kt\mu_b\left[1 + \cot(ktN)\cot(\frac{kt}{2N})\right]$$

The above conditions are applied on the surface of the coating and predict the proper surface wave modes. However, they were derived for an infinite layer without the presence of any terminations. Therefore, when applied to the case of a groove having abrupt material terminations at x=0 and x=w, we expect that the simulation provided by (30) in conjunction with (32) and (33) will not be as accurate. As a result, the GIBC must be supplemented by additional (more accurate) conditions at the terminations of the coating or in this case the groove. At this point, no standard methodology has

been devised for imposing these supplementary conditions, but in either case such conditions will be specific to the geometrical and material properties of the termination. Before, however, we examine the issue of supplementary conditions, let us first proceed with a direct implementation of the third order GIBC noted above. It will be seen that comparison of the results obtained via a direct application of this GIBC will guide us on how these can be supplemented at the terminations.

For H_z polarization, $H_y = 0$, and thus the relevant GIBC is (30a). Expanding this we have

$$\left(a_0 - \frac{a_2}{k^2} \frac{\partial^2}{\partial y^2} \right) E_y + \left(- \frac{a_1}{jk} + \frac{a_3}{jk^3} \frac{\partial^2}{\partial y^2} \right) \frac{\partial E_y}{\partial y} = 0 \; ; \quad y = 0^+ \tag{34}$$

To introduce the equivalent magnetic current $M_z = E_x$ in (34), we note that

$$\nabla \cdot \vec{E} = 0 \tag{35}$$

and thus

$$\frac{\partial E_y}{\partial y} = - \frac{\partial E_x}{\partial x} = - \frac{\partial M_z}{\partial x} . \tag{36}$$

Substituting (36) into (34) now yields

$$\frac{j}{4} \left[a_0 + \frac{a_2}{k_0^2} \left(k_0^2 + \frac{\partial^2}{\partial x^2} \right) \right] \int_0^w 2M_z (x') \frac{\partial}{\partial x} H_0^{(2)} (k \mid x - x' \mid) \, dx' \; +$$

$$+\frac{1}{jk_o}\left[a_1+\frac{a_3}{k_o^2}\left(k_o^2+\frac{\partial^2}{\partial x^2}\right)\right]\frac{\partial M_z(x)}{\partial x}=\left(a_0-\frac{a_2}{k_0^2}\frac{\partial}{\partial y^2}\right)2Z_0\cos\phi_0\,H_z^i \quad (37)$$

In deriving (37) we also employed the wave equation

$$\frac{\partial^2 E_y}{\partial y^2}=-\frac{\partial^2 E_y}{\partial x^2}-k_o^2 E_y \quad (38)$$

and have set

$$E_y=E_y^i+E_y^r+E_y^s=-2Z_o\cos\phi_o\,H_z^i+E_y^s \quad (39)$$

where

$$E_y^s=-\frac{j}{4}\int_0^w 2M_z(x')\,H_0^{(2)}(k_o|x-x'|)\,dx' \quad (40)$$

is the y component of the scattered field in which the factor of 2 is due to image theory.

Integrating both sides of (37) with respect to x eliminates one of the derivatives. Doing so, we obtain

$$\left[1+\frac{a_2}{a_0}\left(1+\frac{1}{k_0^2}\frac{\partial}{\partial x^2}\right)\right]\frac{k_o Y_o}{2}\int_0^w M_z(x')\,H_o^{(2)}(k_o|x-x'|)\,dx'+$$

$$+\left[\frac{a_1}{a_0}+\frac{a_3}{a_0}\left(1+\frac{1}{k_0^2}\frac{\partial^2}{\partial x^2}\right)\right]Y_o M_z(x)=2\left[1+\frac{a_2}{a_0}\left(1+\frac{1}{k_0^2}\frac{\partial^2}{\partial x^2}\right)\right]e^{jk(x-\frac{w}{2})\cos\phi_o} \quad (41)$$

and we note that for $a_2 = a_3 = 0$ (41) reduces to the SIBC integral equation (28) provided the identification noted in (31) is also employed.

The integral equation (41) derived by imposing the GIBC lends itself to a solution via the CGFFT method. Defining the fourier transform pair

$$\tilde{G}(k_x) = \mathcal{F}\{G(x)\} = \int_{-\infty}^{\infty} G(x)\, e^{-jk_x x}\, dx \tag{42}$$

$$G(x) = \mathcal{F}^{-1}\left\{\tilde{G}(k_x)\right\} = \int_{-\infty}^{\infty} \tilde{G}(x)\, e^{jk_x x}\, dk_x \tag{43}$$

we have

$$\mathcal{F}\left\{H_o^{(2)}(k_o|x|)\right\} = \tilde{H}_o^{(2)}(k_o|x|) = \frac{2j}{\sqrt{k_x^2 - k_o^2}} = \frac{2j}{k_o\sqrt{f_x^2 - 1}} \tag{44}$$

($\sqrt{-1} = j$) and by recalling the convolution theorem

$$\int_0^w M_z(x')\, H_0^{(2)}(k_o|x - x'|)\, dx' = 2j\, \frac{\tilde{M}_z(k_x)}{k_o\sqrt{f_x^2 - 1}} \tag{45}$$

since $M_z(x)$ is zero outside $0 < x < w$. Also, in the transform domain

$$\frac{\partial}{\partial x} \rightarrow jk_x, \quad \frac{1}{k_o^2}\frac{\partial^2}{\partial x^2} \rightarrow -\frac{k_x^2}{k_o^2} = -f_x^2$$

and (41) may thus be written as

$$\mathcal{F}^{-1}\left\{\left[\frac{j}{\sqrt{f_x^2-1}}+\frac{\frac{a_1}{a_0}+\frac{a_3}{a_0}(1-f_x^2)}{a+\frac{a_2}{a_0}(1-f_x^2)}\right]\tilde{M}_z(k_x)\right\}=2Z_o\,e^{jk(x-\frac{w}{2})\cos\phi_o} \qquad (46)$$

A CGFFT implementation of (46) is a straightforward task and typical results as computed by (46) are shown in fig. 4. As expected, the third order GIBC applied to the groove, predicts reasonably well the exact magnitude and phase of the current distribution when away from the termination of the groove. The accuracy of this prediction, of course, depends on the depth of the groove, t, and the material properties of the dielectric filling. Our preliminary investigation indicates that for lossless dielectrics, the above third order GIBC provides a reasonable prediction of the current distribution away from the groove terminations for $kt \leq 1$. However, for lossy dielectrics substantially deeper grooves can be simulated.

Next, we consider a hybrid GIBC-exact formulation to alleviate the difficulties of the GIBC in predicting the currents near the groove terminations.

IV. HYBRID GIBC-EXACT FORMULATION

The GIBC formulation in conjunction with the CGFFT solution method offers the substantial advantage of having an O(N) menory requirement. However, as seen in Fig. 4, the current distribution predicted by the third order GIBC is not of acceptable

accuracy when within 0.2 wavelengths of the groove terminations or so. To alleviate this difficulty, one approach is to feed the currents predicted by the GIBC integral equation (41) away from the edges into the exact integral equation (20). The last can then be solved for the remaining currents in the vicinity of the groove terminations. This only requires the inversion of a small matrix thus alleviating the usual difficulties with storage.

Suppose now that $M_z^G(x)$ denotes the current computed via the GIBC integral equation given in (41) and likewise $M_z^e(x)$ denotes the current computed via the exact integral equation. Employing $M_z^G(x)$ in place of $M_z(x)$ in (20) for $x_\Delta < x < w - x_\Delta$ yields

$$\frac{k_o Y_o}{2}\left\{\int_0^{x_\Delta} M_x^e(x')\, H_o^{(2)}(k_o|x-x'|)\,dx' + \int_{w-x_\Delta}^{w} M_z^e(x')\, H_o^{(2)}(k_o|x-x'|)\,dx'\right\}$$

$$-j\frac{k_b Y_b}{w}\sum_{p=0}^{\infty}\frac{\varepsilon_p}{k_p \tan(k_p t)}\cos\frac{p\pi x}{w}\left\{\int_0^{x_\Delta} M_z^e(x')\cos\frac{p\pi x'}{w}\,dx' + \int_{w-x_\Delta}^{w} M_z^e(x')\cos\frac{p\pi x'}{w}\,dx'\right\}$$

$$= 2e^{jk(x-\frac{w}{2})\cos\phi_o} - \frac{k_o Y_o}{2}\int_{x_\Delta}^{w-x_\Delta} M_z^G(x')\, H_o^{(2)}(k_o|x-x'|)\,dx'$$

$$+\frac{jk_b Y_b}{w}\sum_{p=0}^{\infty}\frac{\varepsilon_p}{k_p \tan(k_p t)}\cos\frac{p\pi x}{w}\int_{x_\Delta}^{w-x_\Delta} M_z^G(x')\cos\frac{p\pi x'}{w}dx'. \qquad (47)$$

Assuming that $M_z^G(x)$ has already been determined via a CGFFT solution of (46), the entire right hand side of (47) is known. Thus for $x_\Delta \leq 0.25$ a 4x4 or a 6x6 square impedance matrix is required for the solution of $M_z^e(x)$. In general, continuity of the current density must also be imposed at the transition regions between $M_z^G(x)$ and $M_z^e(x)$.

The results shown in figure 5 clearly show that the proposed hybrid formulation can provide an accurate prediction of the scattering by a groove. The bistatic and backscatter echowidths presented in the course of the above developments have been summarized in Fig. 6. Other examples for the current distributions and corresponding echowidths are given in figures 7 - 11. In these figures the following labeling has been employed

EXACT: Data from a numerical implementation of the exact integral equation (20).

SIBC: Data from a CGFFT implementation of (46) with $a_3 = a_2 = 0$ and in conjunction with (31)

condition.

GIBC-3: Data from a CGFFT implementation of the integral equation (46) resulting from the third order generalized impedance boundary condition.

Hybrid-1: Data from the hybrid SIBC-exact formulation.

Hybrid-3: Data from the hybrid GIBC-exact formulation employing the 3rd order GIBC.

V. CONCLUDING REMARKS

An application of a third order generalized boundary condition (GIBC) to scattering by a two dimensional dielectrically filled cavity was considered. In the process of examining the accuracy of the GIBC, an exact solution was developed and a solution based on the standard impedance boundary condition (SIBC) was examined. An analytical comparison of the integral equation based on the SIBC with the exact, revealed the well known limitations of the SIBC formulation. It was concluded that the SIBC integral equation will, at most, generate an average of the actual current distribution provided the groove is very shallow.

The GIBC integral equation was found easier to implement. Furthermore, unlike the exact integral equation, it was amenable to a conjugate gradient FFT solution and is, thus, attractive for three dimensional implementations. It was found to predict the correct current behavior reasonably well away from the terminations of the groove particularly for lossy dielectric fillings. However, the inadequacy of the GIBC formulation near the groove terminations proved problematic. The GIBC conditions needed supplementation in these regions and several approaches were examined to correct their deficiency. Our initial hope was that the addition of filamentary currents at the edges would provide the required correction as was already done in the case of an isolated thin dielectric layer. This approach, however, was not found suitable for the subject geometry. Instead, the incorrect currents near the groove terminations were replaced with those computed via the exact integral equations. Specifically, the currents computed via the GIBC formulation away from the groove termination were

employed in the exact integral equation to generate a small 4x4 or a 6x6 matrix for the currents in the vicinity of the terminations. This was referred to as a hybrid exact-GIBC approach and was found to provide a reasonably good simulation of lossy dielectric fillings at all angles of incidence and observation. In case of lossless and low contrast dielectrics, the simulation was adequate for groove depths up to 3/20 of a wavelength.

References

[1] T.B.A. Senior, "Approximate Boundary Conditions," IEEE Trans. Antennas and Propagat., Vol. AP-29, pp. 826-829, 1981.

[2] T.B.A. Senior and J.L. Volakis, "Derivation and Application of a Class of Generalized Impedance Boundary Conditions," accepted in IEEE Trans. Antennas and Propagat.; see also University of Michigan Radiation Laboratory report 025921-1-T.

[3] S.N. Karp and Karal, Jr., "Generalized Impedance Boundary Conditions with Application to Surface Wave Structures," in *Electromagnetic Wave Theory*, part I, ed. J.Brown, pp. 479-483, Pergamon: New York, 1965.

[4] A.L. Weinstein, *The Theory of Diffraction and the Factorization Method*, Golem Press: Boulder, Co., 1969.

[5] J.L. Volakis and T.B.A. Senior, "Diffraction by a Thin Dielectric Half Plane," IEEE Trans. Antennas and Propagat., Vol. AP-35, pp. 1483-1487, 1987.

[6] J.L. Volakis, "High Frequency Scattering by a Thin Material Half Plane and Strip," Radio Science, Vol. 23, pp. 450-462, May-June 1988.

[7] J.L. Volakis and T.B.A. Senior, "Application of a Class of Generalized Boundary Conditions to Scattering by a Metal-Backed Dielectric Half Plane," Proceedings of the IEEE, May 1989; see also University of Michigan Radiation Laboratory report 388967-6-T.

[8] D.T. Auckland and R.F. Harrington, "Electromagnetic Transmission through a Filled Slit in a Conducting Plate of Finite Thickness, TE Case," IEEE Trans. Antennas and Propagat., Vol. AP-26, No. 7, pp. 499-505, July 1978.

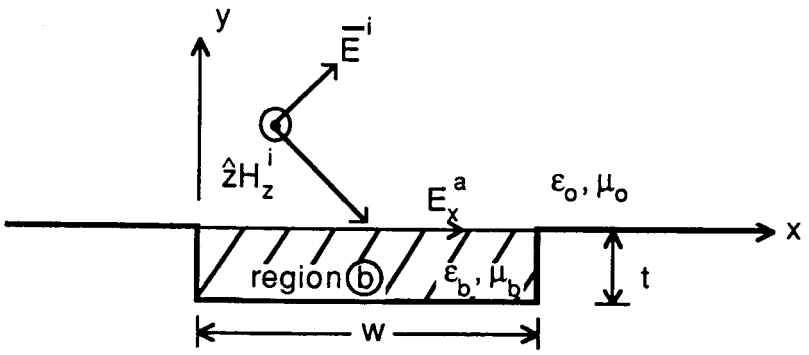

Fig. 1. Geometry of the rectangular groove in a ground plane

Equivalence Principle : $\bar{M} = \bar{E} \times \hat{n}$, $M_z = E_x$

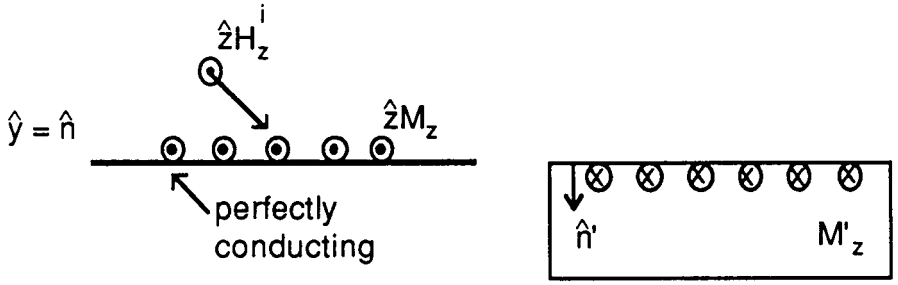

Image theory :

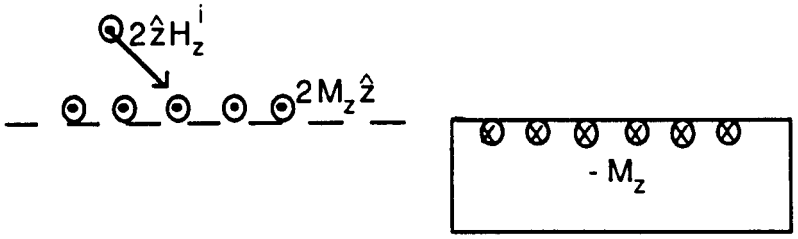

Fig. 2. Illustration of the application of equivalence and image theory.

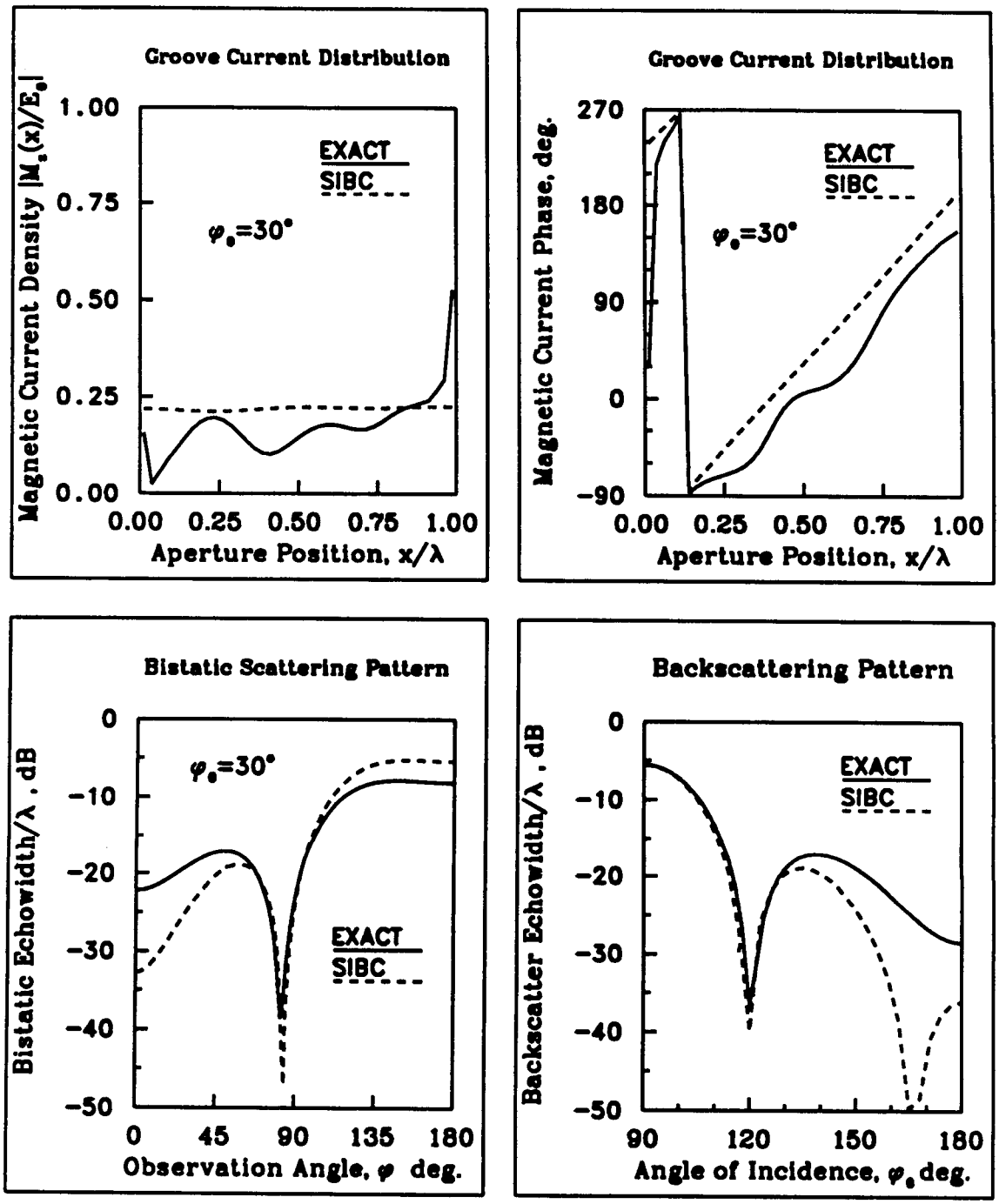

Fig. 3 Comparison of results for scattering from a groove obtained by the exact and the SIBC formulations; groove width w=1λ, depthb=0.2λ, ε_b=7.0−j1.0, μ_b=1.

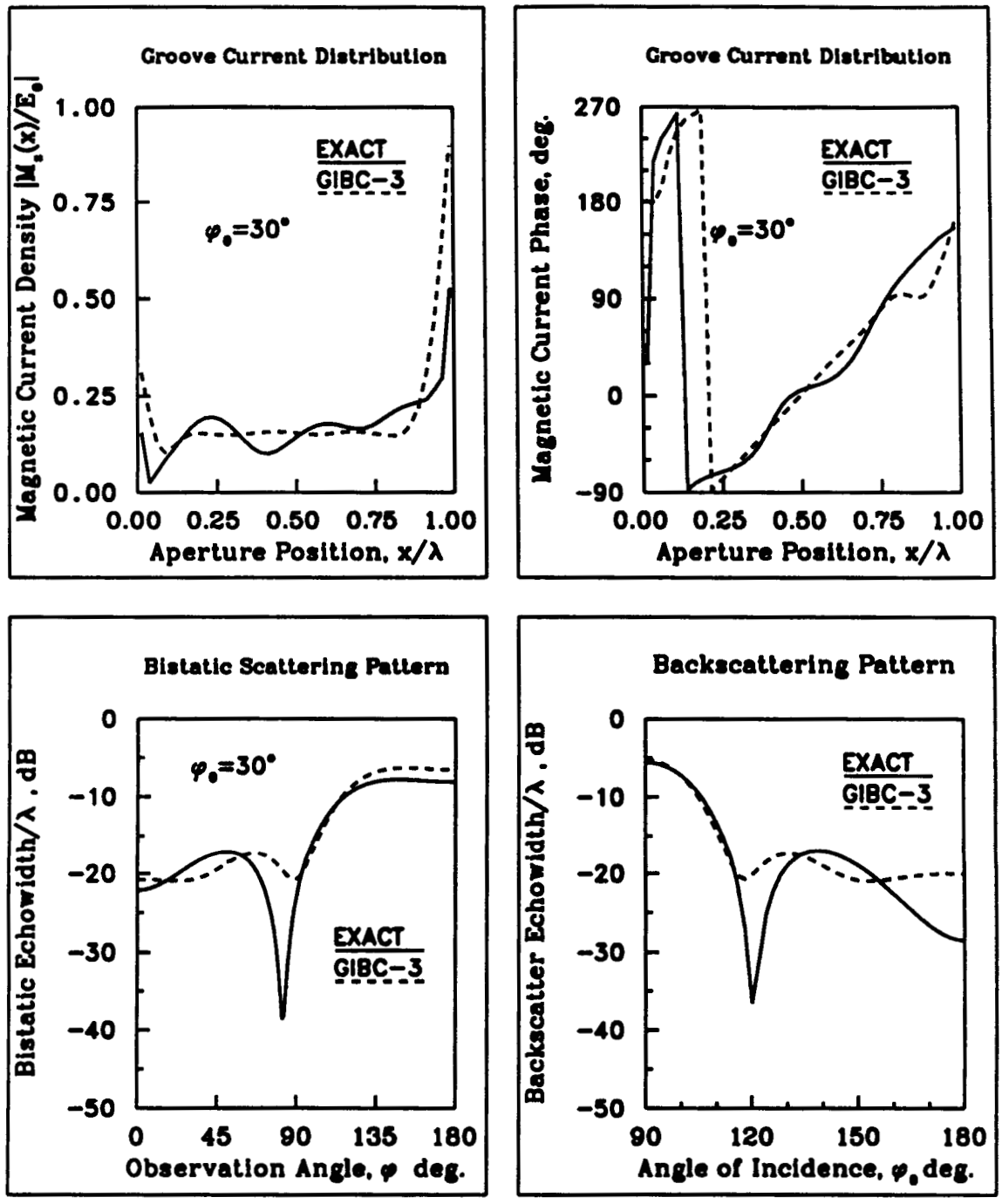

Fig. 4 Comparison of results for scattering from a groove obtained by the exact and the third order GIBC formulations; groove width w=1λ, depth t=0.2λ, ε_b=7.0−j1.0, μ_b=1.

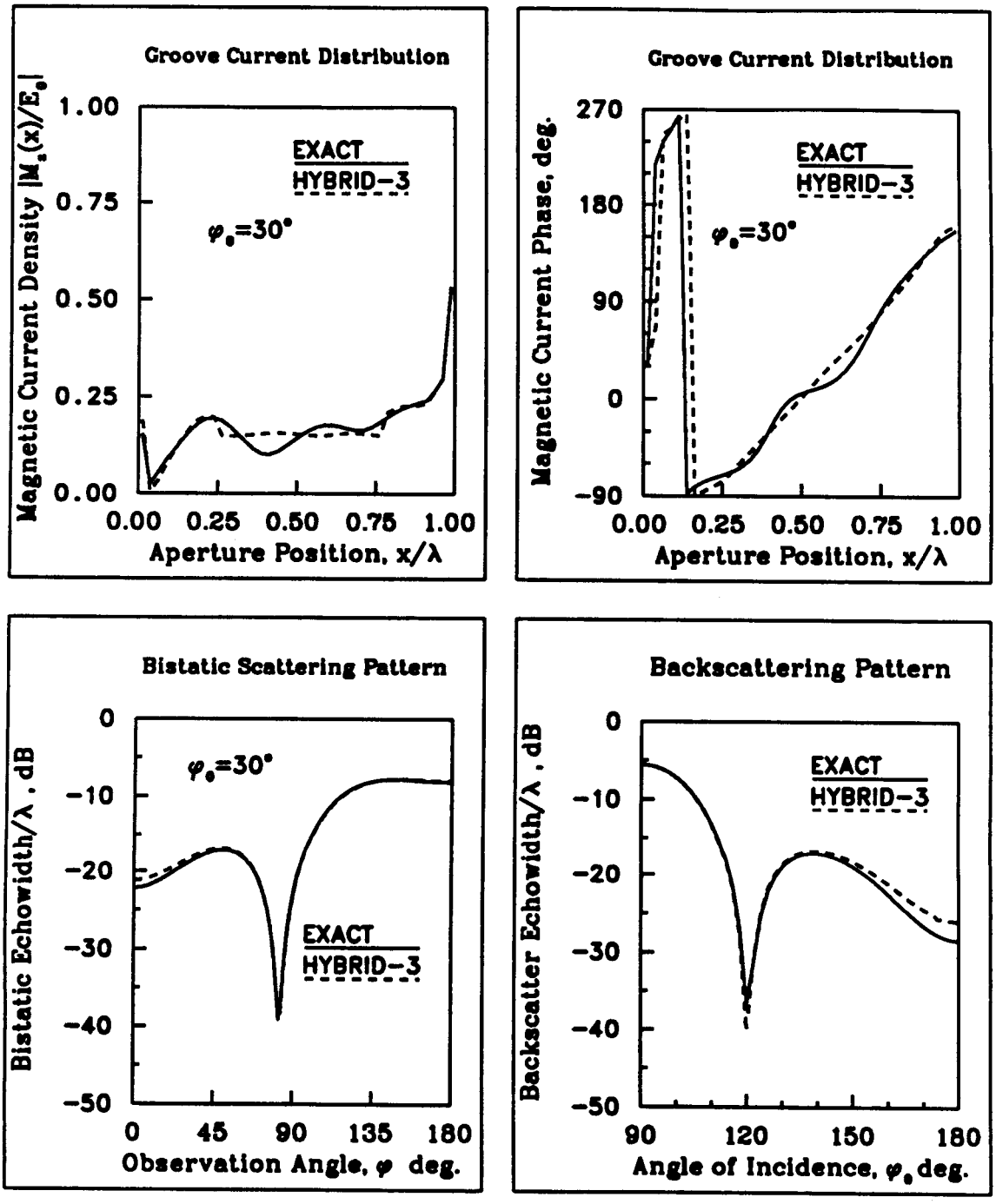

Fig. 5 Comparison of results for scattering from a groove obtained by the exact and the hybrid GIBC formulations; groove width w=1λ, depth=0.2λ, ε_r=7.0−j1.0, μ_r=1.

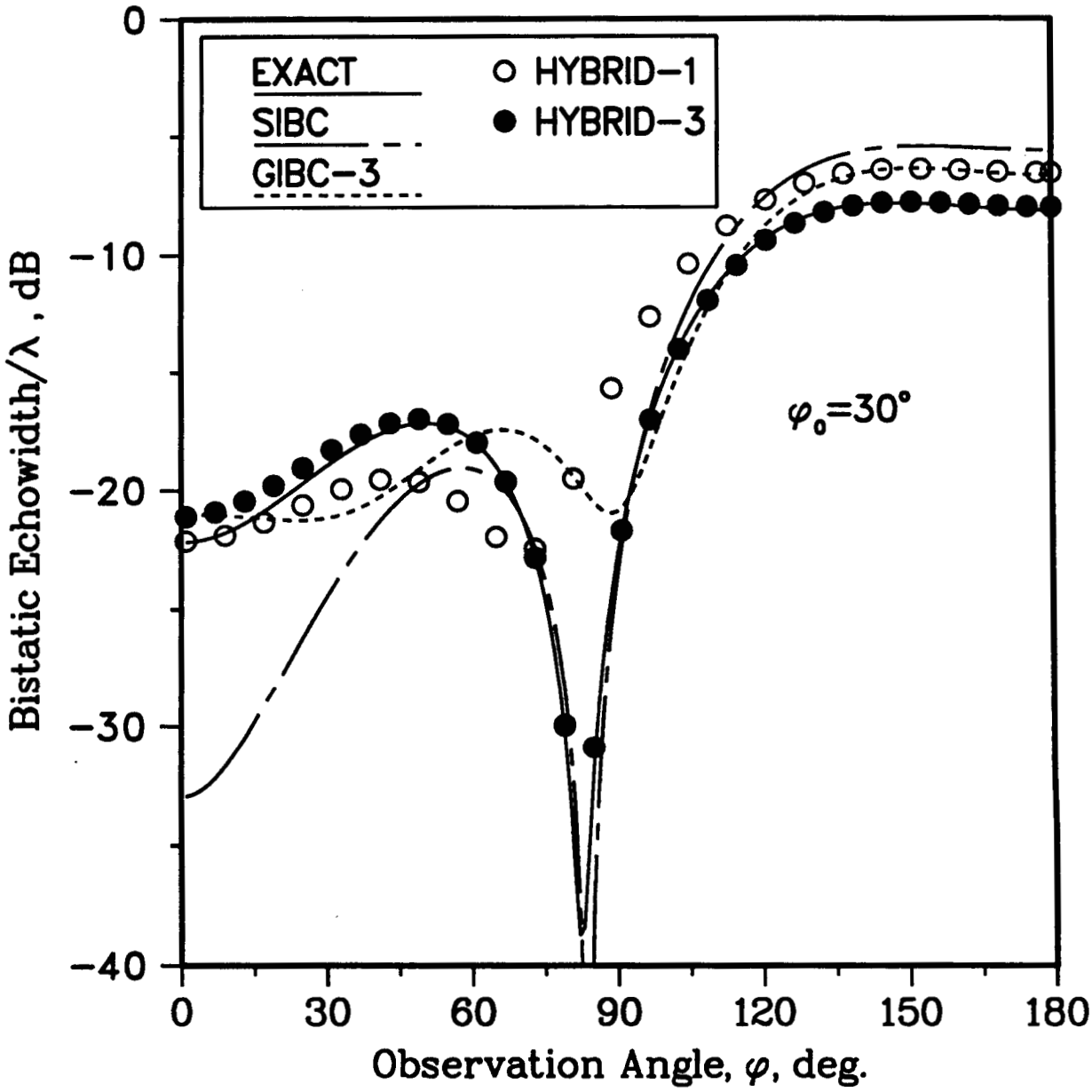

Fig. 6(a) Comparison of bistatic scattering patterns obtained by different formulations as indicated; w=1λ, t=0.2λ, ε_b=7.0−j1.0, μ_b=1.

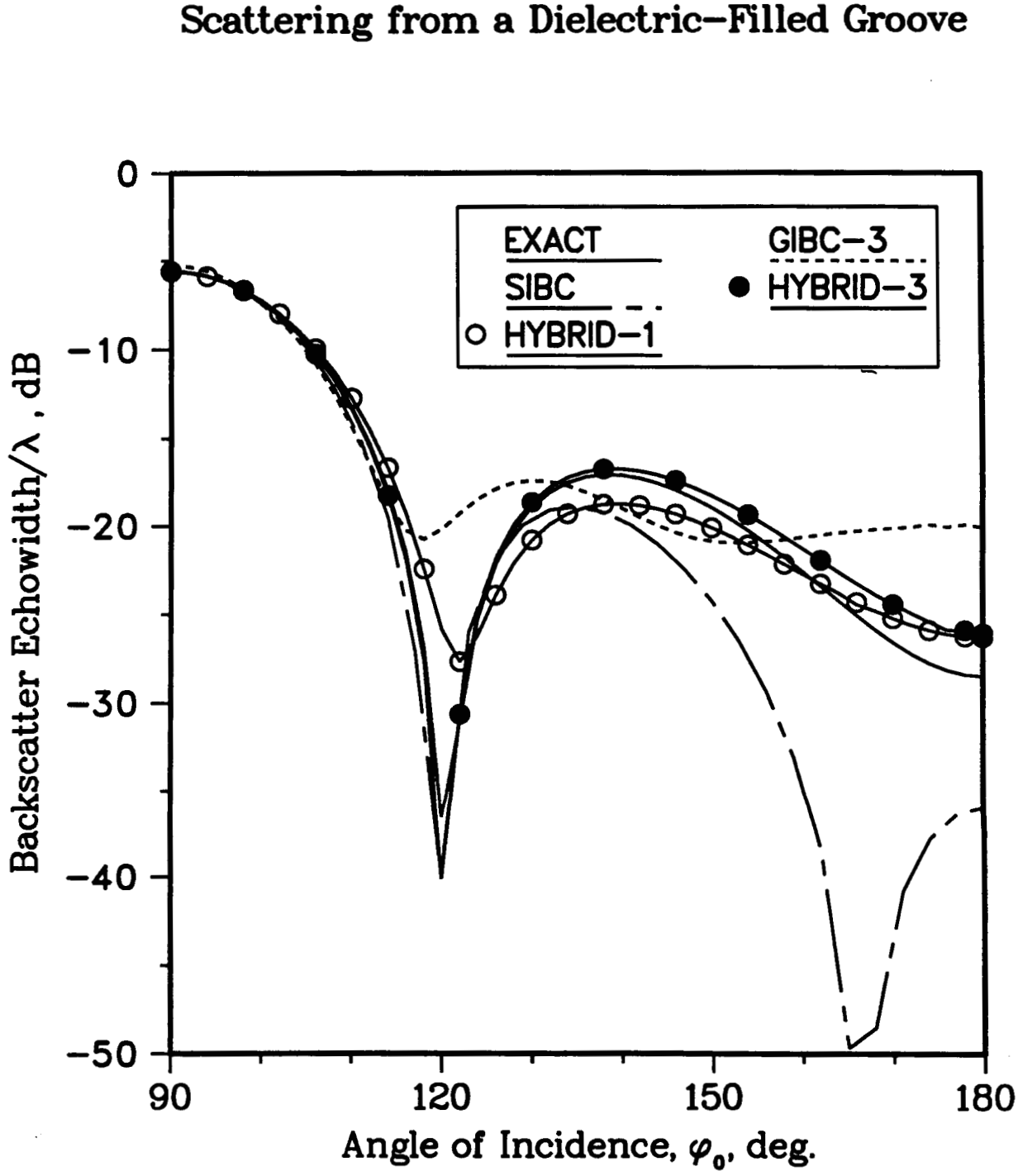

Fig. 6(b) Comparison of backscattering patterns obtained by different formulations as indicated; w=1λ, t=0.2λ, ε_b=7.0–j1.0, μ_b=1.

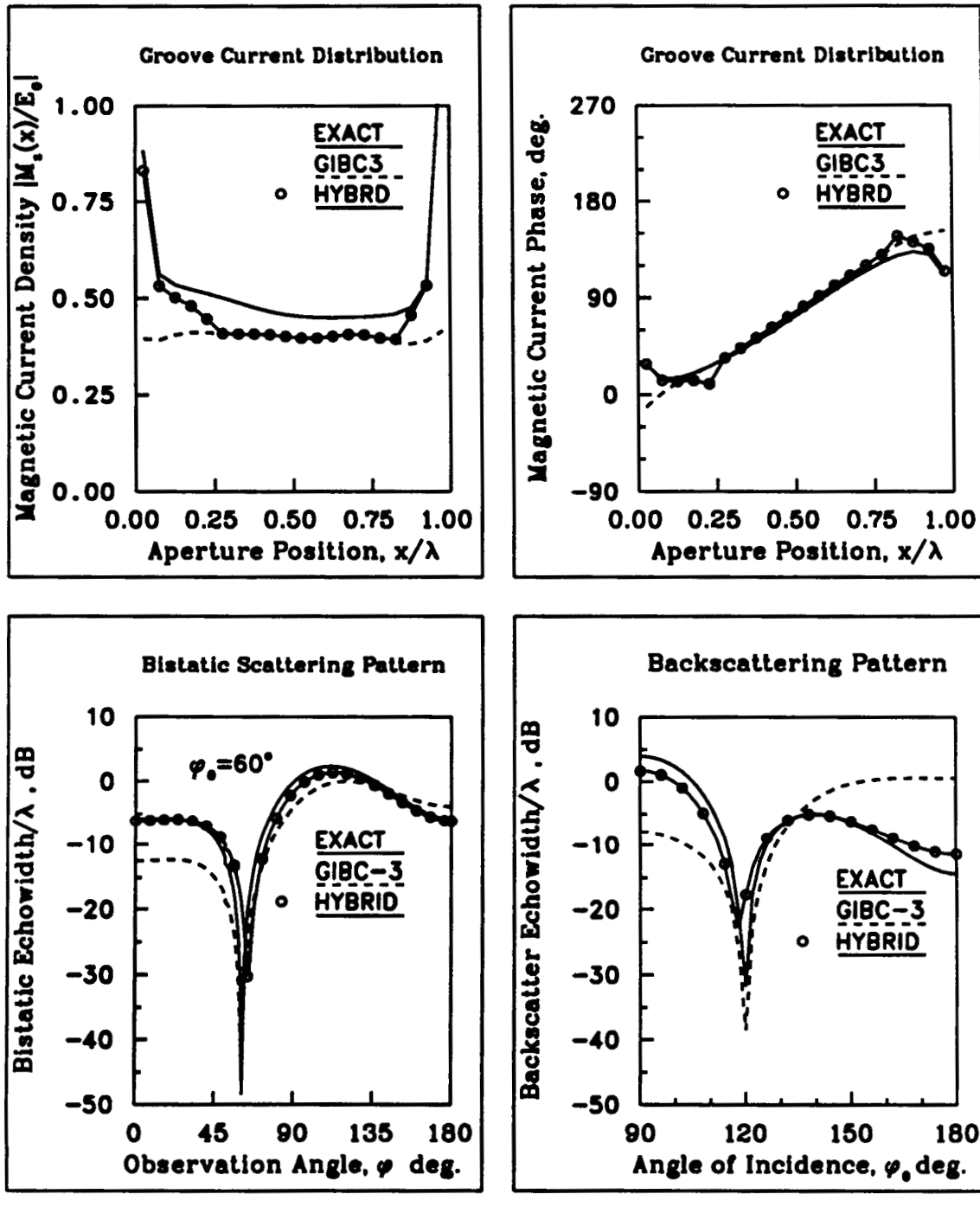

Fig. 7 Comparison of results for scattering from a groove obtained by the exact, third order GIBC alone and hybrid formulations; groove width $w=1\lambda$, depth $t=0.05\lambda$, $\varepsilon_b=1$, $\mu_b=1$.

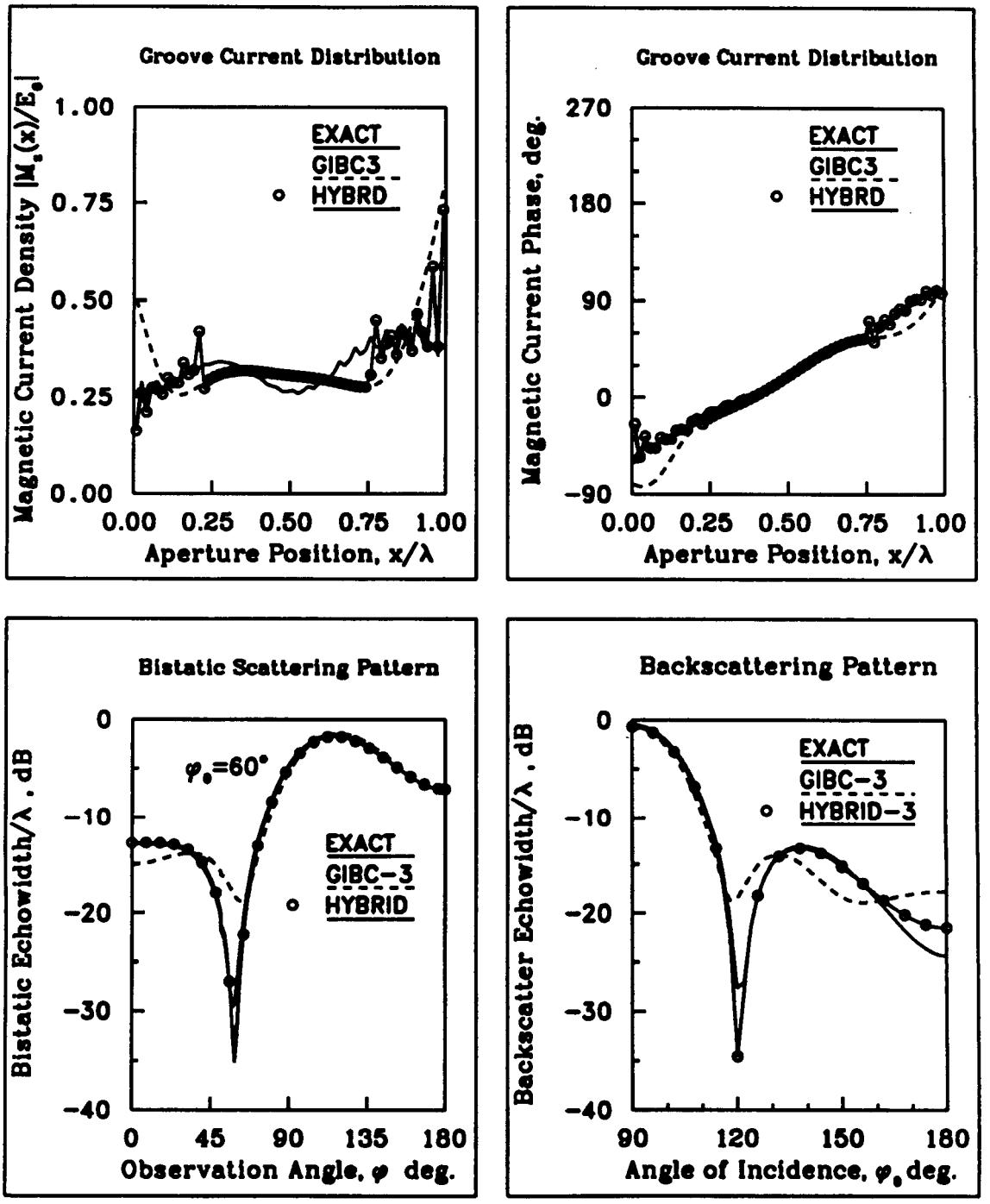

Fig. 8 Comparison of results for scattering from a groove obtained by the exact, third order GIBC alone and hybrid formulations; groove width w=1λ, depth t=0.4λ, ε_r=7.0−j1.0, μ_r=1.

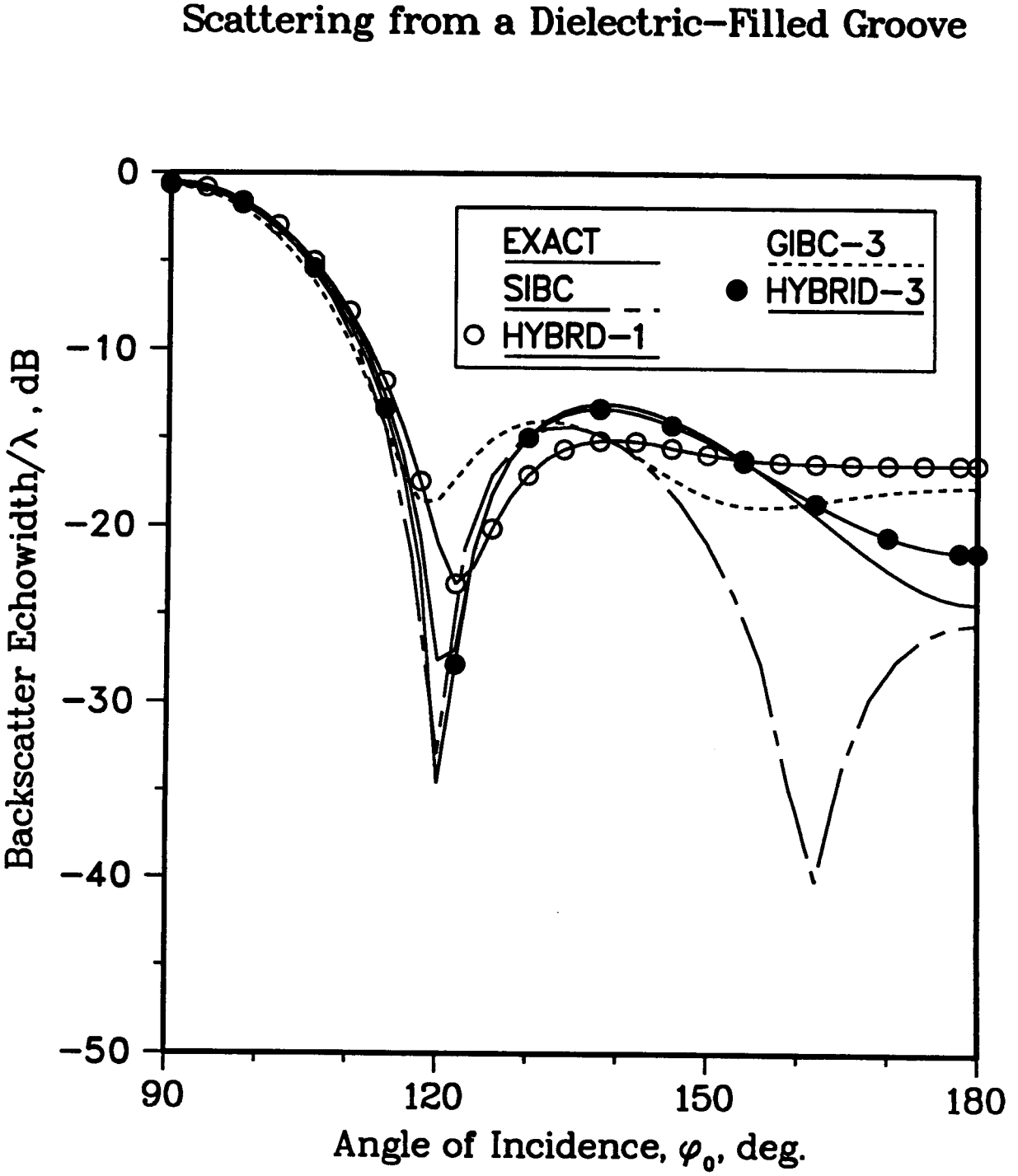

Fig. 9 Comparison of backscattering patterns obtained by different formulations as indicated; w=1λ, t=0.4λ, ε_b=7.0-j1.0, μ_b=1.

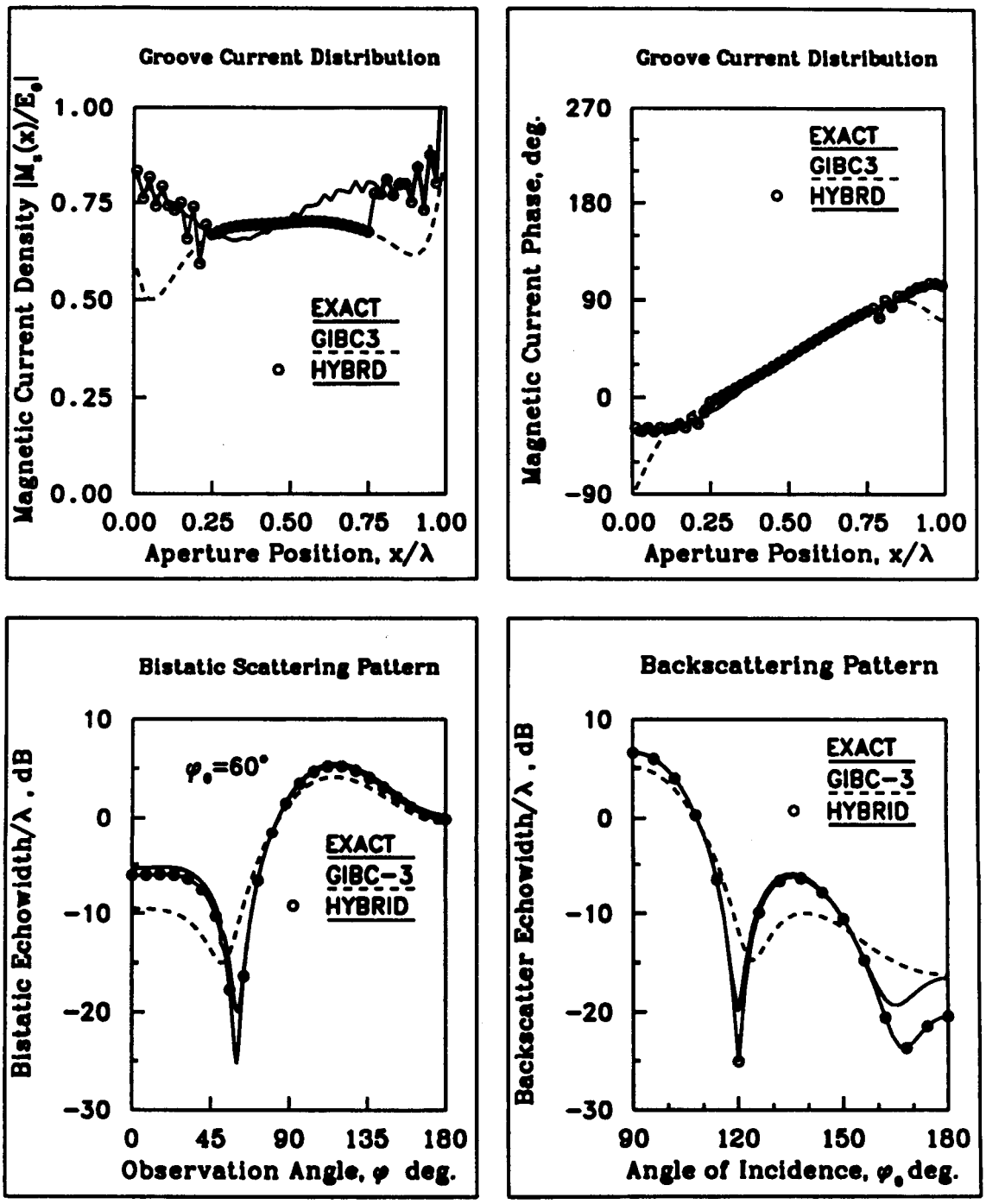

Fig. 10 Comparison of results for scattering from a groove obtained by the exact, third order GIBC alone and hybrid formulations; groove width w=1λ, depth t=0.25λ, ε_r=7.0−j1.0, μ_r=1.